Investigation of Winding Schemes by slot-based High-Frequency Modelling of a Hairpin Winding Stator

Silvan Scheuermann[1], Martin Doppelbauer[1], Björn Hagemann[2], Antoine Jarosz[2], Felix Hoffmann[1]

[1]*Institute of Electrical Engineering (ETI) Karlsruhe Institute of Technology (KIT), Kaiserstr. 12, 76131 Karlsruhe, Germany*
[2]*Delta Electronics (Netherlands) B.V. , Werner von Siemens Str. 2 6, Building 5161, 76646 Bruchsal, Germany*
silvan.scheuermann@kit.edu

Keywords: AC machines, Electric machines, Impedance measurement, Insulation, Voltage measurement

Abstract

The winding insulation system of inverter-fed electrical machines is exposed to electrical stress due to unpredictable transient overvoltages. The voltages in the µs range happen with fast switching inverters and high DC link voltages. These high-frequency voltage overshoots can cause partial discharges and further lead to severe damage to the machines' insulation systems, bearings which result in a reduction of their lifetime. In the present study, a high-frequency hairpin stator lumped parameter model in a slot-based domain was developed and the influence of a winding scheme on such overvoltages was investigated. The parameters for the model have been calculated analytically or were derived from impedance measurements. The generation of simulation models with different winding schemes was automated and a beneficial winding scheme was determined.

1 Introduction

High efficiency, high power density, and low maintenance cost are only a few benefits of Permanent Magnet Synchronous Motors (PMSM). For traction motor applications, hairpin winding technology with a large conductor cross-section has attracted growing international attention and has already been widely used, for example in Toyota's Prius or Porsche Taycan [1], [2]. In traction applications, inverter-fed adjustable speed drives combined with pulse width modulation (PWM) are state of the art [3], [4]. The use of fast switching insulated gate bipolar transistors (IGBTs) and metal oxide semiconductors (MOSFETs), especially the use of silicon carbide (SiC) and gallium nitride (GaN) materials, leads to high du/dt at the motor terminals. Due to parasitic capacitances and inductances, existing in electrical machines in general, propagation paths for electromagnetic interference (EMI) emissions, induced by the inverter, are provided [4]. Such conducted EMI emissions can cause many damaging effects. For example, Common Mode (CM) current paths lead to bearing currents, motor insulation stress, and other inference to the systems' environment, which reduce the reliability of such systems. The importance to find measures is obvious, not only relevant in electrical machine windings, but also for transformer systems [5]. The challenging trade-off between efficiency and reliability must be overcome.

Much research has been worked out in the last decades to understand high frequency damaging effects. Time-domain and frequency-domain modelling have been proposed to predict the system's high-frequency behaviour. In early stages, researchers tried to build simple models to estimate electric discharge machining (EDM), overvoltages at the motor terminal, as well as bearing currents [4]. Many of these models are inadequate to analyze the whole high-frequency behaviour for both, Common Mode (CM) and Differential Mode (DM) configuration. An overview of different models at various levels of complexity is given in Table 1 of [5].

Particularly in these HF equivalent models, circuit parameters are calculated by use of the finite element analysis (FEA), others extract from the measured resonant frequencies and curve fitting. However, relying on precise measurements to model all high frequency effects and behaviour is difficult [6]. However, this paper deals with the HF parameter extraction based on a test-based method in combination with an analytical approach and proposes an equivalent circuit corresponding to a lumped parameter approach. The study presents a high-frequency model for a PMSM traction motor with a star connection and a hairpin winding configuration. The proposed model can simulate the DM and CM impedances of the motor with sufficient accuracy over a wide frequency range. The further aim of the model is to investigate different winding schemes regarding the insulation stress and overshoot voltages. The equivalent circuit model can be executed in simulation tools, such as MATLAB/Simulink or LTSpice. In Section 2 the measurement results of CM and DM impedance using Newtons4th PSM3750 impedance analyzer [7] is presented. The derived high-frequency model of the electrical machine is proposed in Section 3, in which the determination of all circuit parameters is demonstrated in detail. The comparison, effectiveness, and validity of the model are demonstrated in the following Section, before in Section 5 alternative winding schemes regarding the maximum voltage overshoots are investigated. Finally, a conclusion is given in the last Section 6.

2 Measurement setup and the stator's impedance characteristic

The impedance analyzer Newtons4th PSM3750 [7] was used to measure the Common Mode (CM) and Differential Mode (DM) impedance of the motor in the frequency range between 1 kHz and 10 MHz. Fig. 1 (a) and Fig. 1 (b) show both configurations.

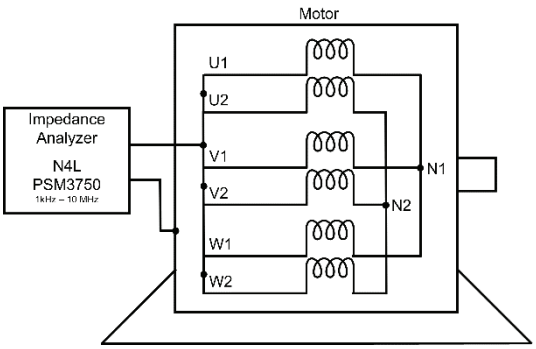

a

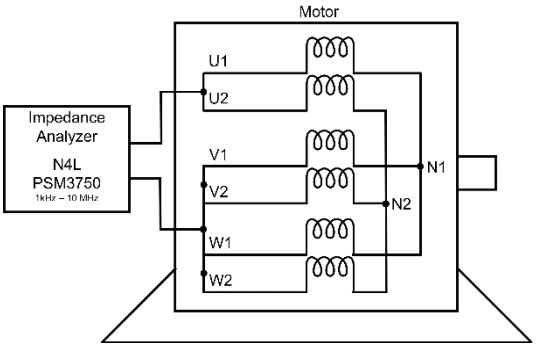

b

Fig. 1: Common Mode (a) and Differential Mode (b) connection configuration

As presented in Fig. 1 (a), the CM impedance was measured by connecting the short-circuited terminals U, V, and W and the motor housing or lamination stack.
The DM impedance measurement (Fig. 1 (b)) is conducted between the terminal of phase U and the other terminals V and W. During the measurements, the motor is disconnected from all other environmental parts and the rotor has not been assembled with the aim to characterize the stator lamination stack and the stator winding only. The magnitude of the measured CM and DM impedance, respectively the phase angle, are presented in Fig. 2 (a) and Fig. 2 (b).
In the low-frequency range, the CM impedance shows capacitive behaviour, which can be easily proved by the phase angle of nearly −90°. Around 1 MHz the first corner frequency can be seen. After this point, the curve can be described neither as capacitive nor as inductive since the phase angle strives to zero before it becomes capacitive again. The high-frequency motor model is also supposed to replicate the resonances in this frequency range. The second resonance point at 10 MHz is also targeted to be simulated. The DM impedance (Fig. 2 (b)) in contrast indicates inductive behaviour, which can be validated by the phase angle of +90°. The first resonance point occurs as well near 1 MHz. Above the resonance, a capacitive behavior becomes dominant and lasts until the measured range of around 10 MHz before a second resonance point appears.

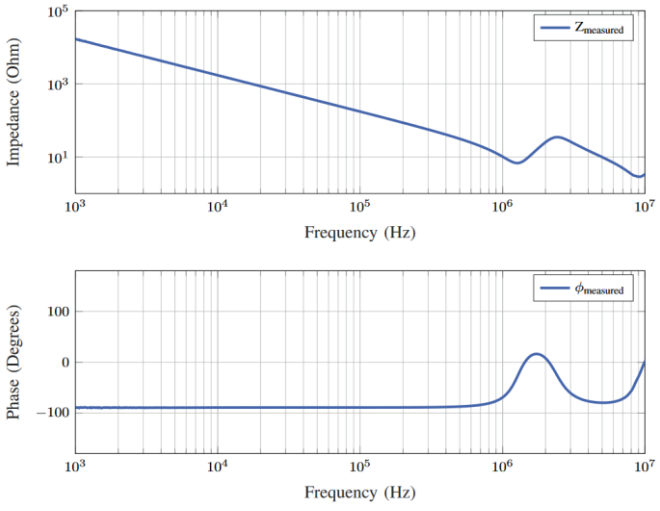

a

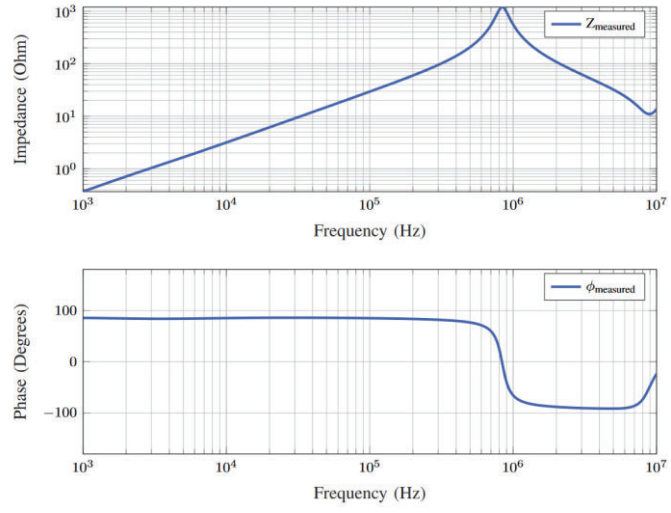

b

Fig. 2: Common Mode (CM) measurement result (a) and Differential Mode (DM) measurement result (b)

3 Development of the simulation model

3.1 Proposed equivalent electrical circuit

The development of a suitable lumped parameter model to simulate the CM- and DM-impedances can be separated into two parts. The first step is the choice of an appropriate equivalent electrical circuit and the second contains the calculation of the necessary parameters for each included element. The basics of the high-frequency model are shown in Fig. 3.

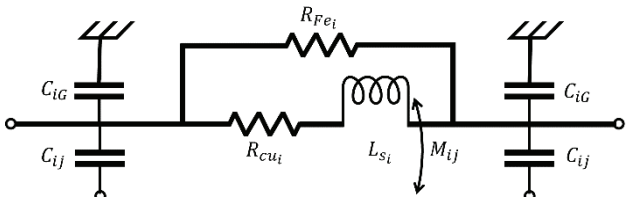

Fig. 3: Single slot level based high-frequency model

Different from other models found in literature, the model of this study is based on a single slot approach. The modeled motor has four coil-sides in each of the 48 slots. The single-slot level based high-frequency model consists of a resistance $R_{cu,i}$ and an inductance $L_{s,i}$ for each coil-side. Furthermore, a mutual inductance M_{ij} between two coil-sides in one slot is considered.
For symmetry reasons, the equivalent circuit model is equipped with two capacitances C_{iG} and C_{ij} for the whole stack length, which can be considered in the parameter calculation. These elements describe the parasitic capacitances between the winding and the stator lamination stack C_{iG} and C_{ij} those between the coil-sides in each slot. All elements used in the simulation model are assumed to be ideal without any frequency dependency. For the sake of simplicity and because separation of the influence of the windings'overhang from measurement data is not possible, the resistance and inductance values are already considered in the parameters of the slot itself.

3.2 Circuit parameter determination

The parameters for each element of the model have been calculated analytically from geometric data or extracted by an impedance measurement of the stator in the respective frequency range between 1 kHz and 10 MHz. Out of this range, the measurements are not usable because of strong measurement noise. As a consequence of the necessity of constant parameters in LTSpice, the parameters, extracted from measurements, have been matched with the phase angle first and then averaged over the respective frequency range. The properties of the stators' windings are summarized in Table 1.

Table 1 Circuit parameter determination

Number of slots	N	48
Number of phases	m	3
Number of pole pairs	p	4
Number of layers	n_L	4
Number of parallel paths	n_{pp}	2

3.2.1 Resistance R_{cu} :

At low frequencies, the impedance is dominated by the DC resistance of the copper coils, which is given by the conductivity of the copper material. In combination with the specific resistivity ρ and the geometric data of the strand, the calculation of the resistor-value for the slot and overhang part is possible with Eq. (1).

$$R_{cu} = \rho \cdot \frac{l_{slot,overhang}}{A_{coil}} \quad (1)$$

In the overhang part, the shapes and lengths of the hairpin coil differ. In dependence of position and side (crown- or welding-side), the calculation has been executed.

3.2.2 Stator winding resistance R_{fe} :

The modeled stator-winding resistance R_{fe} has been derived from the CM Measurement at the resonance point at $f_{res,CM}$= 1.27 MHz. It can be assumed that at this frequency, the impedance is dominated by R_{fe} and the remaining components of the slot are negligible. This assumption results in a parallel connection of all stator-winding resistances and the parameter value were calculated by equation Eq. (2).

$$Z_{measured}(f_{res,CM}) = 6.8\,\Omega \quad (2a)$$

$$R_{fe} = N \cdot n_L \cdot Z_{measured}(f_{res,CM}) = 1305.6\,\Omega \quad (2b)$$

3.2.3 Inductance L_s :

The main inductance of the slot-based model has been determined by another frequency-dependent RLC-measurement. These measurements have been conducted with an unwelded stator, so that different hairpin configurations could have been measured. By averaging the measurements and with the use of the Eq. (3b), the value of the inductance was determined.

$$Z_{imag} = \omega \cdot L_s \quad (3a)$$

$$L_s = \frac{Z_{imag}}{2 \cdot \pi \cdot f} = \begin{cases} 2 \cdot 587.125\,\text{nH} & \text{for } L_{s1}, L_{s2} \\ 2 \cdot 495.198\,\text{nH} & \text{for } L_{s3}, L_{s4} \end{cases} \quad (3b)$$

The calculated value for the inductances corresponds to two coil-sides. Therefore, the half value must be considered for the model on a single slot level.

3.2.4 *Mutual inductance M_{ij}:*

The coupling coefficients between two inductances L_i and L_j within one slot were calculated based on an energy conversion approach and coefficient comparison according to [8]. It was assumed that coupling occurs only between coil-sides of one slot. The coupling coefficients are printed in Table II, the respective mutual inductance can be calculated by Eq. (4).

$$M_{ij} = k_{ij} \cdot \sqrt{L_i \cdot L_j} \quad (4)$$

When selecting the simulation software, care was taken to include the coupling factors occurring between the inductances of each layer, which is a big benefit of LTSpice.

Table 2 Coupling coefficient of inductances in one slot

Coupling coefficient k_{ij}	Value (-)
k_{12}	0.818
k_{13}	0.672
k_{14}	0.583
k_{23}	0.880
k_{24}	0.764
k_{34}	0.910

3.2.5 *Capacitance C_{iG} and C_{ij}:*

Both parasitic capacitances must be considered - for the strands to the stator lamination stack C_{iG} and between the coil sides C_{ij} within a slot. For this purpose, non-adjacent strands can be neglected, since only a very small capacitance is formed due to the relatively large distance. This simplification can be verified by an electrostatic FEM-simulation or seen in [9].
For the capacitance calculation, the neighbouring areas A, the distance d, and the relative permittivity ε_r of the insulation material of the motor are required in each case.
For parallel surfaces with constant permittivity of the material between two surfaces, the capacitance can be calculated by Eq. (5).

$$C = \varepsilon_0 \cdot \varepsilon_r \cdot \frac{A}{d} \tag{5}$$

The formula is applicable for capacitances between the strands C_{ij} and for all strand-stator capacitances C_{iG} apart from the conductor located at the slot opening.
At this point, neither the distance nor the permittivity of the intervening material remains constant because part of the volume is filled with air and the slot opening is bevelled. To calculate this capacitance C_{40}, the average distance of the slopes to the conductor was calculated and the relative permittivity of air ε_r = 1 was included. Finally, the values are presented in Table 3.

Table 3 Coupling coefficient of the inductances in one slot

Capacitance C	Magnitude (pF)
C_{10}	96.7
C_{20}	54.7
C_{30}	54.7
C_{40}	71.4
C_{12}	20.8
C_{23}	20.8
C_{34}	20.8

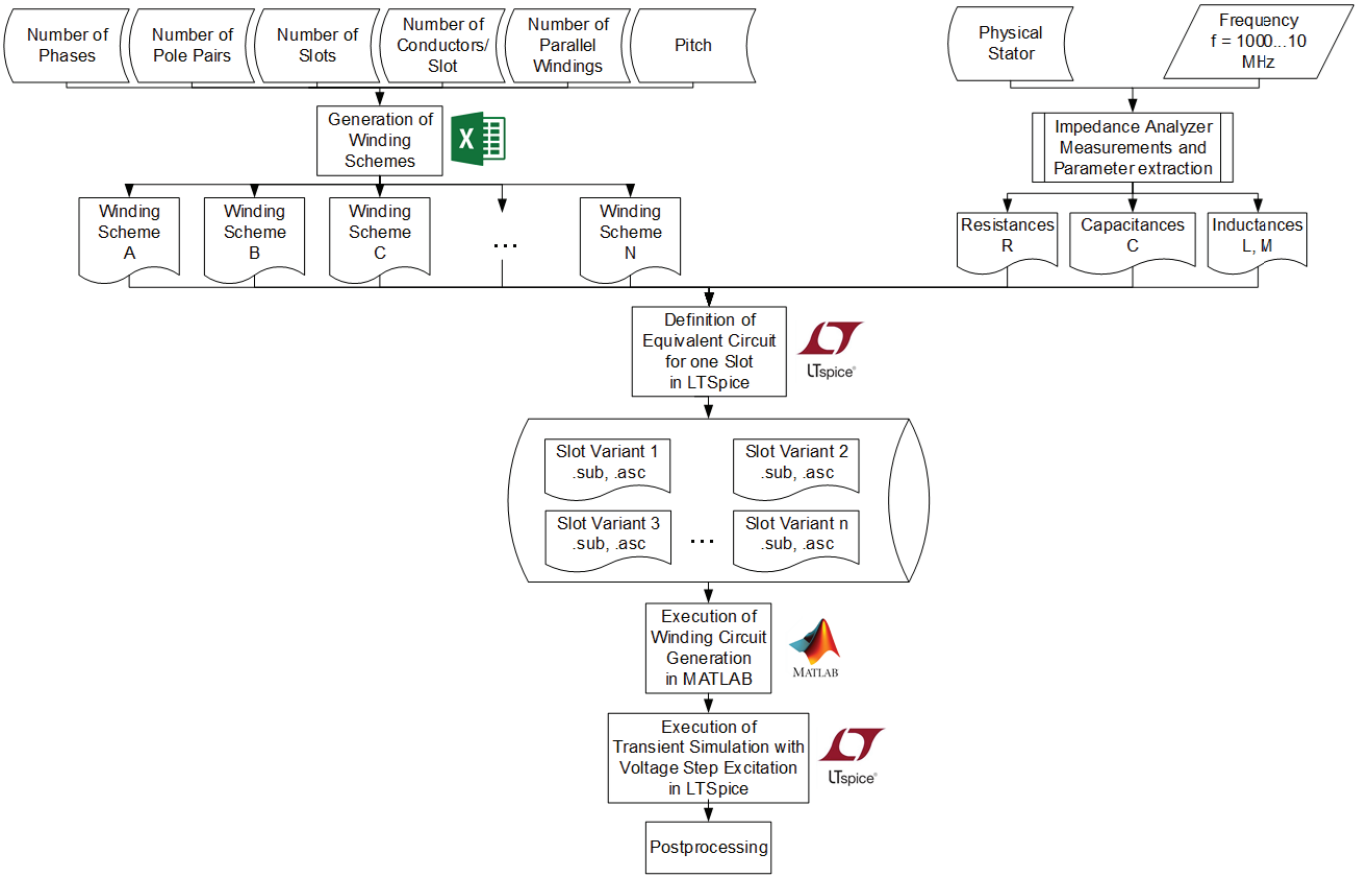

Fig. 4: Simulation process

3.3 Implementation in LTSpice

The simulation model of the stator was built by a self-deployed automated algorithm. Subcircuits were created for one slot and subsequently called from the component library. These have terminals for the crown-side and welding-side, whose number corresponds to the number of conductors per slot per slot. In addition, a terminal for the stator lamination stack was introduced so that the DM configuration with its floating stator lamination stack potential can also be implemented.
Depending on the winding scheme, the subcircuits of the slots were interconnected. Since the influence of the overhang was already considered in the slots, the connection between the slots is modeled as an ideal connection. For the different configurations DM and CM, the terminals on the stator terminals are assigned differently (see Figs. 1(a) and 1(b)). The voltage source in the model is not only used for the impedance analysis, it is also applicable to simulate a transient voltage pulse or step excitation, which corresponds to the switching behavior of semiconductors. This extension opens the possibility to simulate the transient voltage stress of the insulation material in the time domain. The impedance analysis in LTSpice is modeled by a sinusoidal excitation of different frequencies. By dividing the voltage U by the current I, the impedance Z in the frequency-domain is depictable.

3.4 *Automated generation of simulation models*

Regarding the aim, to investigate a variety of different winding schemes, the generation of the simulation models with different winding configurations has been automated. After developing different winding schemes and storing them in tabular form, other input information like the number of slots N, strands per slot z_N, phases m, and the number of parallel paths a of one phase must be given. By defining an appropriate subcircuit for one slot only once, an LTSpice netlist will be created. This netlist contains all information about the nodes and the connection between the strands of different slots and their position within, thus all information about the overhangs' design. A summary of the whole process is given in Fig. 4.

4 Simulation and experimental result

With the calculated parameters of the high-frequency model of the tested hairpin stator, the DM and CM impedances have been simulated in LTSpice. Fig. 5 shows both, the amplitude and phase angle of the measured and simulated CM impedance**.**
A peculiarity is given by the fact that a slot-based model was developed, not comparable to the models found in literature [4]-[6]. The impedance of the model fits quite well with the measured one over the whole frequency range, which indicates that the model is valid for further transient voltage investigations and other CM effects occurring in motors. The model also has largely enhanced the DM characteristic at the whole frequency range and covers the resonance points (see Fig. 6).

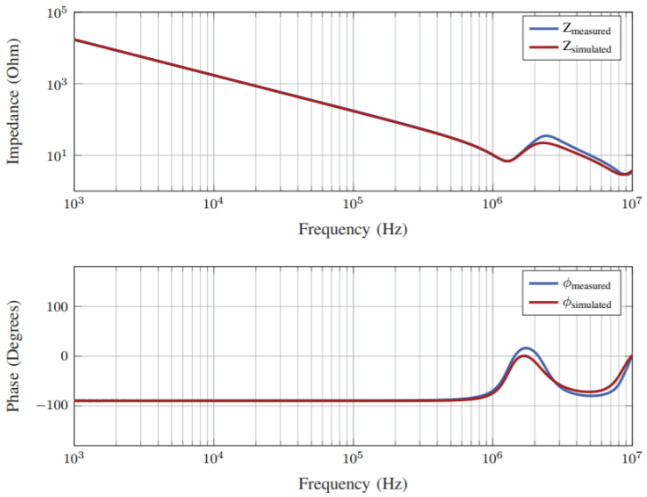

Fig. 5: Measured and modeled common mode impedance

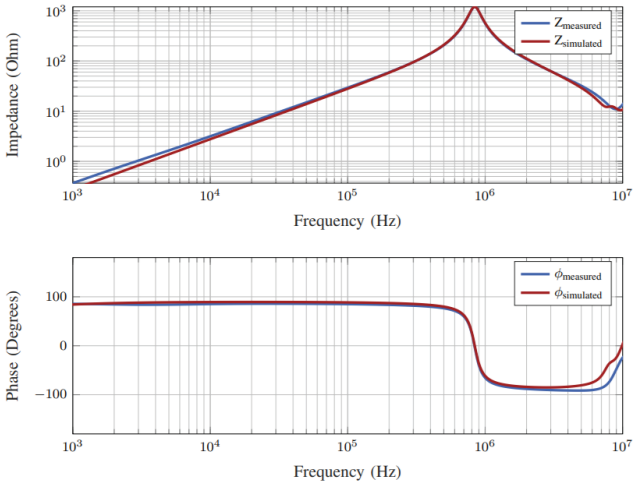

Fig. 6: Measured and modelled differential mode impedance

Besides CM, also major DM effects in the physical stator can be represented. Minor deviations in the high-frequency range can be accepted since interference in the measurements cannot be guaranteed to be non-existent.
In general, the overall agreement of the model is still good and suitable for predicting transient effects. Further, it should be used to show the influence of different winding schemes under the assumption, that the slot-based strand parameters remain constant.

5 Application to an alternative winding scheme

The previously presented methodology, extensively summarized in Fig. 4 has been applied to different winding schemes. The simulation and the following investigation of the voltage stress have been conducted in Differential Mode configuration. In Fig. 7, the simulated transient voltages $U_{C,i}$ of the coils at different winding positions are presented.

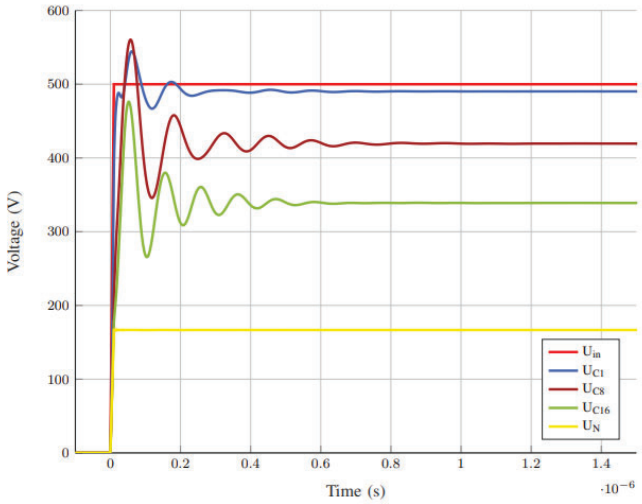

Fig. 7: Simulated voltages of the coils $U_{C,i}$ at different winding positions

It can be seen, that in two different winding schemes (WS), the maximum voltages are increasing first with also increasing position in direction to the neutral point, positioned at coil number 32.

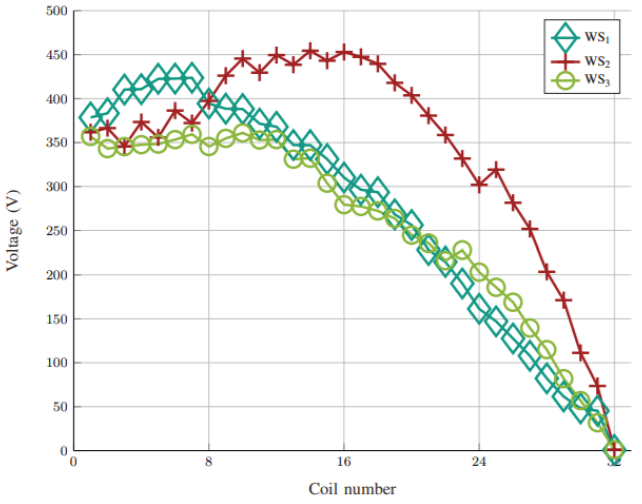

Fig. 8: Maximum voltage $U_{C,i}$ of different winding schemes

6 Conclusion

A high-frequency model for a hairpin winding stator on a slot-based approach is proposed in this study. All parameters of the model have been either derived from CM or DM impedance measurements or were analytically calculated. The comparison between the simulated and measured impedance shows good accuracy. Hence, the model can be directly applied in simulation tools to calculate high-frequency harmonic components and can be used further to simulate transient voltages in the time domain. This opens the possibility to simulate the voltage stress of the stator windings, but also can identify critical voltage stress areas. Further, a determination of an alternative winding scheme with beneficial properties regarding the motor insulation material is possible. The following work, based on this study, must conclude the validation of the time domain voltage simulations by measurements, but also the calculation of the lumped parameters on the basis of geometric data, e.g. with the help of numerical or analytical approaches. The ultimate goal of identifying high-frequency effects and insulation stress in motors in early motor design stages can be reached with the help of such a slot-based lumped equivalent circuit model.

7 References

[1] S. Sano, T. Yashiro, K. Takizawa, and T. Mizutani, 'Development of new motor for compact-class hybrid vehicles,' World Electric Vehicle Journal, vol. 8, no. 2, pp. 443-449, 2016.

[2] Porsche AG, 'Antrieb: Performance pur,' https://newsroom.porsche.com/de/produkte/taycan/antrieb-18543.html, accessed 25 February 2022.

[3] T. M. Jahns, G. B. Kliman, and T. W. Neumann, 'Interior permanent magnet synchronous motors for adjustable-speed drives,' IEEE Transactions on Industry Applications, vol. IA-22, no. 4, pp. 738-747, 1986.

[4] Y. Wu, H. Li, W. Ma, M. Dong, and Q. Zhong, 'High-frequency model of permanent magnet synchronous motor for emi prediction in adjustable speed drive system,' in 2018 IEEE International Power Electronics and Application Conference and Exposition (PEAC). IEEE, 2018, pp. 1-6.

[5] A. Hoffmann and B. Ponick, 'Method to predict the non-uniform potential distribution in random electrical machine windings under pulse voltage stress,' Energies, vol. 15, no. 1, p. 358, 2022.

[6] Y. Ryu, B.-R. Park, and K. J. Han, 'Estimation of high-frequency parameters of ac machine from transmission line model,' IEEE Transactions on Magnetics, vol. 51, no. 3, pp. 1-4, 2015.

[7] Newtons4th, 'PSM3750 Frequency Response Analyzer,' https://www.newtons4th.com/products/impedance-analysis-interface-2/, accessed 25 February 2022.

[8] J. Staszak, 'Determination of slot leakage inductance for three-phase induction motor winding using an analytical method,' Archives of Electrical Engineering, vol. 62, no. 4, pp. 569-591, 2013.

[9] G. Berardi, S. Nategh, and N. Bianchi, 'Inter-turn voltage in hairpin winding of traction motors fed by high-switching frequency inverters,' in Proceedings 2020 International Conference on Electrical Machines (ICEM). IEEE, 2020, pp. 909-915.